

**NASA TECHNICAL  
MEMORANDUM**

NASA TM X-52289

NASA TM X-52289

FACILITY FORM 802

**N 67 - 27 238**  
(ACCESSION NUMBER)

21  
(PAGES)

TMX 52289  
(NASA/CR OR TMX OR AD NUMBER)

\_\_\_\_\_  
(THRU)

1  
(CODE)

28  
(CATEGORY)

**M-1 INJECTOR DEVELOPMENT - PHILOSOPHY  
AND IMPLEMENTATION**

by William A. Tomazic, E. William Conrad,  
and Thomas W. Godwin

Lewis Research Center  
Cleveland, Ohio

GPO PRICE \$ \_\_\_\_\_

CFSTI PRICE(S) \$ \_\_\_\_\_

Hard copy (HC) \$ 3.00

Microfiche (MF) .65

ff 653 July 65

TECHNICAL PAPER proposed for presentation at Third Propulsion  
Joint Specialists Conference sponsored by the American  
Institute of Aeronautics and Astronautics  
Washington, D. C., July 17-18, 1967

**NATIONAL AERONAUTICS AND SPACE ADMINISTRATION : WASHINGTON, D.C. : 1967**

**M-1 INJECTOR DEVELOPMENT - PHILOSOPHY AND IMPLEMENTATION**

by William A. Tomazic, E. William Conrad, and Thomas W. Godwin

Lewis Research Center  
Cleveland, Ohio

**TECHNICAL PAPER** proposed for presentation at

**Third Propulsion Joint Specialists Conference**

sponsored by the American Institute of Aeronautics and Astronautics

Washington, D. C., July 17-18, 1967

**NATIONAL AERONAUTICS AND SPACE ADMINISTRATION**

## M-1 INJECTOR DEVELOPMENT - PHILOSOPHY AND IMPLEMENTATION

William A. Tomazic, E. William Conrad, and Thomas W. Godwin  
Lewis Research Center  
National Aeronautics and Space Administration  
Cleveland, Ohio

### Abstract

The injector design was a cooperative effort between Aerojet-General Corporation and the Lewis Research Center with the goal being to achieve high performance with completely stable operation. The approach was based on the technology already established in the RL-10 and J-2 engine development programs, supplemented with the latest data obtained at LeRC. Small-scale tests were conducted at LeRC to verify the design concepts prior to incorporation into the full-scale hardware.

Full-scale injector testing demonstrated that the design goals were achieved. A combustion efficiency of 96 percent at 5.5 mixture ratio was achieved. Vacuum specific impulse, extrapolated from the basic test data to intended engine conditions was approximately 430, which is just above the PFRT goal. The injector was highly resistant to both hydraulic and acoustic instabilities. No instabilities of any kind were experienced at rated conditions. Low level "chugging" occurred during the start transient only. Acoustic instability was not encountered until hydrogen injection temperature was reduced below 80°R. Stable operation was restored by raising the hydrogen temperature to 100°R, indicating a substantial margin even under conditions of extreme perturbation (engine design operating temperature is 142°R).

### Introduction

Injector development has historically been a prolonged, iterative process. The basic difficulty has been one of avoiding combustion instability, while at the same time achieving high combustion performance. This problem has become more severe as engine size has increased. Lack of basic knowledge on instability, its prevention and cure, has generally forced injector development along the tortuous path of "cut and try" with little, if any, rational basis.

The M-1 injector was designed with the intent of circumventing the "normal" development route by using all pertinent technology to obtain the "end product" in the initial design; that is, an injector combining high performance, stable operation and durability. The design was a cooperative effort between the engine contractor (Aerojet-General Corporation) and the Lewis Research Center. The primary design goal was to achieve high performance (greater than 96 percent combustion efficiency) with completely stable operation. In addition, mechanical integrity and compatibility with the chamber were required. The design approach was based on the technology already established in the RL-10 and J-2 engine development programs, supplemented with the latest research data obtained at LeRC. Where possible, aspects of the design were finalized and proven through small scale tests. Four specific areas, the injector proper, the injector baffles, the ablative chamber, and the start system were all subjected to intensive design analysis and/or sub-

scale testing prior to commitment to the full scale design.

This paper describes the design approach, the methods of implementation, and the actual hardware developed. The results from full scale thrust chamber testing are presented and compared to corresponding data obtained from subscale testing. The advantages and limitations of subscale testing are discussed.

### Injector Development

#### Background

An assessment of the current state of hydrogen-oxygen injector technology in late 1964 indicated that the J-2 injector design was the most appropriate base to start from in designing the M-1 injector. The coaxial tube injector had by then become essentially "standard" for hydrogen-oxygen; both the RL-10 and J-2 used it. The RL-10 development had not encountered acoustic instability during its development primarily due to its high hydrogen injection temperature and small size. Accordingly, no useful data on suppression of acoustic instability were available from the RL-10 effort. The larger J-2, however, did encounter acoustic instability and techniques for its suppression were developed.

It was found that increasing hydrogen velocity (or momentum) and/or decreasing oxygen velocity resulted in greater stability. In designing coaxial injectors, this was accomplished by reducing hydrogen injection area and increasing oxygen injection area. LeRC research in this area showed the ratio of hydrogen velocity to oxygen velocity to be a significant correlating parameter, with an increased velocity ratio resulting in greater stability. In evaluating the stability of a specific injector, hydrogen velocity was varied by varying hydrogen injection temperature. This approach to stability evaluation has been used extensively both at LeRC and at Rocketdyne for the J-2 development. The LeRC developed method used for the M-1 was to begin at a temperature well above anticipated stability limits, then to ramp temperature down by increasing the proportion of liquid hydrogen entering the mixer and simultaneously reducing the gaseous hydrogen. Figure 1 (ref. 1) shows hydrogen temperature at transition to unstable operation as a function of injection area ratio. Regardless of hydrogen temperature, transition for this particular injector occurred at a velocity ratio of approximately 6.5. Higher velocity ratios resulted in stable operation, lower ratios in instability.

Another significant effect was recessing of the oxygen tube below the face. For the J-2, a recess of 0.210 inch resulted in a 20° to 25° reduction in self-triggering temperature and a 2 percent increase in combustion performance. Figure 2 shows data obtained at LeRC for a 0.1 inch recess. Self-triggering temperature was improved

by approximately 50° and performance by 3 to 4 percent. Both the high velocity ratio and recess techniques enhanced mixing and atomization of the coaxial propellant streams, and resulted in improvements in both stability and performance. The J-2 flight rating test injector (figure 3) employed both effectively.

These same techniques were incorporated into the M-1 injector design. Hydrogen velocity and velocity ratio were made as high as practical within the engine pressure budget. Both oxygen and hydrogen pressure drops were set at a high level to prevent chugging instability. This was done based on a single dead time approach to chugging analysis which specified that increases in either or both pressure drops tended to improve stability. As with the J-2, an element inlet restriction was used to obtain the required oxygen pressure drop for chugging stability and yet allow low oxygen injection velocity for better acoustic stability.

#### Subscale Testing

Subscale tests of the injector element design chosen were undertaken to:

1. confirm performance expectations
2. check susceptibility to chugging instability
3. check on general durability of injector elements and faceplate
4. examine acoustic instability characteristics

The subscale testing effort, including tests of other M-1 element configurations, is reported in detail in reference 3. The testing was carried out at 15,000 lb. thrust, the highest thrust possible at 1040 psi chamber pressure in the LeRC Rocket Engine Test Facility. The subscale injector (figure 4) was 5.4 in. in diameter and contained 51 elements as compared to 40 in. and 3248 elements for the full-scale injector. The full-scale combustor was duplicated exactly in the following aspects:

1. element size and detail
2. chamber pressure (1040 psia)
3. element spacing
4. chamber length (29 in. to throat)
5. contraction ratio (1.7)
6. Rigimesh face porosity
7. faceplate attachment

Figure 5a shows the element with a straight bore liquid oxygen tube; figure 5b with a 7° taper ream at the tip of the LOX tube. The taper ream was added to decrease the LOX velocity and hence increase the hydrogen-oxygen velocity ratio. This particular technique was demonstrated as effective in the work of reference 1. However, the lower LOX velocity prompted some concern about chugging instability. Therefore, both configurations were tested to determine the effect of the modification on chugging and on performance. There were some minor differences in the several non-tapered elements tested, but they apparently did not affect the performance.

A heavy wall carbon steel chamber with a coating of .018 in. of zirconia over .012 in. of nichrome was used. Most of the testing was done

with a chamber 29 in. long from injector to throat. Some tests were made with a 44 in. long chamber to assess possible response of the injector to longitudinal oscillations in the same frequency range as predicted for tangential oscillations in the full-scale chamber.

Combustion efficiency (actual C\* divided by theoretical C\*) of the taper-reamed configuration is plotted in figure 6 as a function of oxidant-fuel ratio for a nominal hydrogen injection temperature of 140°. As noted, two data points at lower chamber pressures were used to extend the curve to mixture ratio extremes. The level is generally very high (98 percent or better) although a slight dropoff of approximately 1 percent occurred between an oxidant-fuel ratio of 4.5 and 6.5.

Figure 7 shows the effect of hydrogen injection temperature on combustion efficiency for both straight and taper-reamed elements. These data are for oxidant-fuel ratios from 4.5 to 6.5. Although some scatter is observed, both injector types maintain approximately 99 percent combustion efficiency from 184°R all the way down to 60°R. No difference was observed in efficiency between the 29 and 44 in. long chambers.

These data (in particular, those showing the effect of H<sub>2</sub> temperature) indicate a very high performance potential for this injector design. Performance for the full scale injector, however, would be expected to be somewhat lower due to the fuel devoted to baffle-cooling (approximately 5 percent) and the peripheral fuel film cooling (approximately 3 percent) intended to protect the regenerative chamber tubes. Rocketdyne experience on J-2 and the data of reference 4 indicate that 8 percent fuel devoted to cooling will decrease injector performance by 1 to 2 percent. It should then be expected that combustion efficiency for the full scale chamber would be approximately 97 percent.

In regard to stability, neither hydraulic or acoustic instability was encountered at or near nominal M-1 operating conditions. Chugging was encountered during many start transients. It should be expected that similar chugging might be encountered on the full scale tests; however, it should not be of consequence due to the low pressures and flows at the time of occurrence. No instances of tangential mode acoustic instability occurred. Four tests with the 44 in. long chamber showed relatively mild longitudinal instability. This was not unexpected, due to the extreme L/D of the chamber. Even then, the only significant instability occurred at conditions of chamber pressure, O/F, and hydrogen temperature far from the normal operating conditions. Table I shows the data for these tests.

FINE ELEMENT INSTABILITY TABULATION

Test No.	Pc Psia	O/F	RIT OR	f Cps	AMP Psi	Mode
216	1007	5.18	66	750	25	1L
217	554	7.47	90	1200	100	2L
218	860	5.93	67	750	20	1L
219	767	5.73	68	1300	35	2L



This run experience was encouraging but not conclusive as far as predicting stable operation for the full-scale chamber.

Throughout the testing, the injector showed excellent durability. No overheating or erosion problems were encountered.

### Full Scale Testing

The full scale injector layout and some of the design details are shown in figure 8. As shown, the chosen baffle layout produced 19 separate injection compartments. The total number of identical elements required to produce the full scale thrust was 3248. The four outer rows of elements were canted towards the chamber center line at  $7^\circ$  to move the point of impingement with the  $11^\circ$  convergent chamber further downstream. This was done because of analysis and previous experience which foresaw a possible chamber erosion problem due to propellant stream impingement on the chamber wall prior to complete combustion.

The first goal of the full scale test effort was to determine performance. The tests were made in an ablative-lined chamber to provide sufficient duration. Thrust, weight flows, pressures, and temperatures were measured to determine performance. Specific impulse and characteristic velocity were derived from the basic data. Characteristic velocity was calculated both from measured specific impulse using an analytically derived thrust coefficient, and from basic parameters ( $P_c$ , weight flows,  $A_T$ ) with analytical correction made for non-isentropic acceleration (momentum pressure loss). The two values agreed within  $1/2$  percent, with the  $C^*$  derived from specific impulse being the lower. Figure 9 shows combustion efficiency vs. oxidant-fuel ratio for both the full scale and subscale testing. Combustion efficiency was calculated using the  $C^*$  derived from specific impulse and the theoretical  $C^*$  for  $140^\circ\text{R}$  hydrogen inlet temperature. The full scale performance at 5.5 O/F was 96 percent of theoretical with a slight increase at lower O/F's and a dropoff at higher O/F's. This performance level met the original goals prescribed for this injector. The subscale data show the same trend with O/F, but are about 3 percent higher. The subscale injector data define a base or ideal level of performance. Deviation from this ideal, as noted earlier, was caused by two factors. First, the full-scale injector devoted approximately 5 percent of its fuel flow to baffle cooling and 3 percent to peripheral film cooling. Data obtained at LeRC and at Rocketdyne on the J-2 program indicate a performance loss of approximately 1 percent for each 4 percent film cooling. This implies a performance loss for the M-1 injector of approximately 2 percent. Furthermore, 748 elements (23 percent) adjacent to the baffles were modified (see baffle section) in order to protect the baffles. Although a precise evaluation of this effect was not made during subscale testing, it is conceivable that a percent or more loss could be attributed to the "dimpling".

Figure 10 shows combustion efficiency as a function of hydrogen injection temperature. Both the full scale and subscale injectors maintain constant efficiency down to low hydrogen temperatures, probably due to the high hydrogen-oxygen velocity ratio. Other work at LeRC has shown that a high velocity ratio is helpful in maintaining a

high efficiency level with decreasing hydrogen temperature (ref. 1). However, the full-scale performance did begin to drop precipitously approximately  $5^\circ$  before the onset of acoustic instability as hydrogen temperature was ramped downward from rated conditions to determine the self-triggering point. This coincided essentially with beginning of a metastable condition prior to full-blown instability.

The performance data obtained at sea level with a 2.08 area ratio nozzle were extrapolated to vacuum conditions assuming a 40 area ratio nozzle. This was done using thrust coefficients determined using a nozzle performance evaluation computer program developed by United Aircraft Corporation. Figure 11 shows the results obtained. The performance at 5.5 O/F (the thrust chamber O/F at engine rated conditions) is 429- $1/2$  seconds which is equivalent to the contract specification for PERT.

The full-scale injector operated stably under all conditions of mainstage, normal operation. Chugging was experienced during the early phases of the staged start transient when injection pressure drops were very low. Chugging pressure amplitudes were approximately 45 psi peak-to-peak during the first phase of the start at 300 psi chamber pressure. The amplitude fell to about 23 psi during the second phase of the start at 450 psi and chugging disappeared completely as the chamber pressure rose further. This is substantially in keeping with the subscale results and indicates a quite stable system.

The next phase of effort was to evaluate the acoustic stability characteristics of the injector. During the performance determination phase of the testing, there was no indication of any acoustic instability, even during the start transient when temperatures dipped below  $80^\circ\text{R}$  and mild chugging was in progress. The method used to induce screaming was to reduce the hydrogen temperature as was done in the subscale testing. The results of this testing are shown in figure 12. Self-triggering temperature (temperature at onset of instability) varied from about  $76^\circ$  to  $81^\circ\text{R}$  with the lower values occurring at low O/F's. During some of the later runs, the temperature was ramped back up after instability began. Return to stable operation occurred at approximately  $100^\circ\text{R}$ . These results indicate a substantial margin even under conditions of extreme perturbation since the engine design operating temperature is  $142^\circ\text{R}$ . When instability was induced, the high frequency pressure pickup data showed no definite mode of instability which is in keeping with some experience with F-1 baffled injectors.

In summary, the original performance goals were met. The injector operated stably under normal conditions of operation and stability evaluation tests at lower hydrogen temperature showed considerable margin.

### Baffle Development

#### Background

Even though every attempt was made in designing the injector itself to utilize the best information on design for stable operation, stability could not be guaranteed because of a lack

of information on scaling. It was decided, therefore, that combustion baffles should be incorporated to further reduce the possibility of deleterious acoustic instability. The actual baffle configuration was designed using the Sensitive Time Lag Theory developed by Crocco and coworkers at Princeton University. Using this analysis technique, it was determined that the most likely modes of oscillation would be the third or fourth tangential with frequencies from 2000 to 3000 cps. The baffle was designed with radial blades to provide protection against spinning tangential modes. Twelve blades were provided around the periphery to preclude standing modes of lower order than the sixth. A ring baffle was provided to eliminate the first radial mode. The analysis is presented in detail in reference 5. Figure 13 shows the selected baffle arrangement. The analysis offered no specific guide as to baffle length; however, past experience led to a choice of 4-inches. It was felt that a 4-inch baffle was long enough to be effective and not so long as to promote inter-cavity modes. (This length was later reduced to 3-1/2 inches based on cooling considerations.)

It was also clear that the baffle must be both adequately and economically cooled. It must perform its function continuously and reliably without substantially compromising the injector performance. Four to six percent of the fuel was chosen as the maximum which would be devoted to baffle cooling without dropping the combustion performance below minimum goals. The most pertinent design information came from the F-1, J-2, and GEMSIP programs. Rigimesh appeared to be a logical first choice for efficient, reliable cooling. However, the generally unsuccessful J-2 experience with Rigimesh baffles was not encouraging. The cooling scheme used for the F-1 copper baffles appeared unsatisfactory because of the much higher heat fluxes for M-1. With no firm precedent for design, it was decided to actually develop the baffle cooling technique at subscale prior to final design of the full-scale baffle.

#### Subscale Testing

The subscale test program was conceived and conducted at the Lewis Research Center using, with some modifications, test set-up and hardware previously used for the injector element investigation. The engine manufacturer contributed strongly to both the concepts and hardware aspects of the subscale program, and also designed the full-scale injector to accommodate readily any baffle concept determined to be optimum in the subscale tests. It was decided to bolt the baffles to the injector to minimize the welding required, and also to provide a quick-change capability in the event that baffle deterioration would be experienced during the full-scale test program.

A cutaway drawing of the subscale engine test assembly is given in figure 14. A separately controlled and metered flow of hydrogen at a temperature of close to 140°R (M-1 design) was supplied through tubes to the base of the baffle. This deviated from the full-scale design where a separate baffle cooling system was not provided and the coolant to the baffle was supplied from the hydrogen injector cavity through holes drilled in the injector faceplate. However, the subscale tests were identical to full-scale in regard to:

1. chamber pressure
2. mixture ratio
3. contraction ratio
4. injector elements
5. element spacing with respect to baffle surfaces
6. element density

Accordingly, and in view of the fact that subscale chamber diameter was not much smaller than the full-scale baffle cavities, the axial heat flux distribution in the vicinity of the baffle is believed to have been closely simulated.

As shown in figure 15, the subscale baffle specimens corresponded to a 2.85-inch slice from one of the six inner spokes of the full-scale baffle. A total of 25 baffle designs were evaluated by gradually reducing the baffle coolant flow until failure occurred. Detailed results are given in reference 6 and only a few of the more significant findings are covered herein.

In the 25 specimens tested, five basic cooling schemes were involved as indicated schematically in figure 16. The baffle types of primary interest herein are the transpiration (type A) and film and convection (type E). The other types assessed were as follows:

Type B - convective cooled: all configurations (copper) showed some erosion near tip but further development could probably achieve successful design.

Type C - reverse flow convection: both .030 copper and nickel stainless steel (electrodeposited) shell configurations met design but showed incipient failure at 75 percent of design coolant flow. Discarded as too complex.

Type D - film cooled: tip erosion of copper tang occurred with film-cooled lengths of 1.5 inches or over.

Early in the subscale investigation, it was found the close proximity of the injector elements to the baffle resulted in LOX-rich propellant stream impingement and consequent erosion. It was found that indenting or "dimpling" the elements immediately adjacent to the baffle would completely relieve this. The "dimpled" elements are shown in figure 17. As discussed earlier, it is likely that this modification effected performance since over 700 elements had to be "dimpled" on the full-scale injector to adequately protect the baffle. A strip of ablative material was used to protect the exposed inner end of the subscale baffle. There were no exposed ends on the full-scale baffle.

Results obtained with the transpiration-cooled baffles are typified by the data of figure 18 where baffle differential pressure is plotted as a function of baffle coolant flow. The shaded region represents the range of values acceptable in the M-1 engine. It is seen that as the baffle coolant flow was reduced from maximum, the baffle pressure drop at first decreased as expected, but then increased rapidly with further reductions of flow below about 0.27 pound per second (equivalent

to 4.5 percent of total fuel flow). At about 0.15 pound per second, a maximum apparently occurred followed by a decrease again toward the origin of the plot. As shown in reference 6, other designs of different porosity and construction did intercept the design region. Nevertheless, all of the transpiration cooled baffles were unacceptable because all exhibited the unexpected "S-shaped" characteristic shown in figure 18.

Operation could occur at any of these regions (A, B or C) for a given injector pressure drop, probably depending upon the sequence of propellant flows during the complex conditions typical of engine start transients. Baffle integrity at B was marginal and damage occurred after two short runs at point C. On the basis of a very cursory analysis, it appeared that the reversal (at 0.27 pound per second in fig. 18) may be associated with sudden disruption of the cool boundary layer normally formed by the emerging coolant on the hot side of the baffle material. Data similar to these had not been found in the prior literature possibly because experiments are not generally carried out to failure and the reversal point was not reached.

A number of type E baffle configurations employing combined convective and film cooling were investigated with tip damage gradually eliminated by detailed modifications. Flow characteristics for the final configuration are shown in figure 19. The full-scale baffle was designed to operate with a total flow of 5 percent of the fuel flow for the injector (subscale baffle flow equivalent to .3 lb/sec). Local areas could be higher or lower depending on injector flow distribution; however, the lowest flow at any point should be equivalent to approximately 4 percent. The subscale baffle was tested at this equivalent flow rate. Only very minor tip damage was sustained (fig. 20a). Another test was made at 80 percent of the lower design flow limit (approximately 3.3 percent equivalent flow rate). Considerably more tip erosion was sustained (fig. 20b). However, it appeared that the baffle had eroded to an equilibrium status and could have maintained its basic structural integrity with further operation. The bolts and seals used in the investigation were designed to full-scale chamber specifications and were found to have adequate structural integrity. This was confirmed both with these hot tests and with shake-table vibration tests using the predicted M-1 engine vibration spectrum.

#### Full-Scale Testing

The full-scale results indicate that the baffles were effective in attenuating instability. Even during induced unstable operation, pressure excursions were limited to 100 to 150 psi peak to peak.

The baffles themselves withstood the rigors of full-scale testing quite well. The inner radial baffles were wholly undamaged, although several erosion spots occurred on the outer circular baffle, and substantial erosion occurred on several of the outer radial baffles. Figure 21 shows the injector and baffles after the first 3 sec. full thrust test at an O/F of 6.12. A subsequent test of 4 sec. at full thrust and 5.34 O/F did not add to the damage. Most of the erosion on the outer radial legs appeared to be due

to inadequate coolant flow. Therefore, after two full thrust tests, the two most severely eroded outer radial legs were replaced with new legs which were redrilled to provide approximately 15 percent greater film coolant flow. Further testing showed substantially less damage to these legs, indicating that the high coolant flow helped.

In general, the bolting of the baffles to the injector proved quite satisfactory. The baffles remained firmly attached with no apparent bolt loosening during stable operation. This confirmed both the sub-scale firings and the shake-table tests. Instability did cause baffle loosening. However, it was not difficult to retighten the baffles as necessary between stability limit tests.

In summary, the subscale development of a baffle-cooling design for the M-1 worked out very satisfactorily. What proved to be a wholly adequate final baffle design was completely established before beginning full-scale tests.

#### References

1. Wanhainen, J. P., Parish, H. C., and Conrad, E. W., "Effect of Propellant Injection Velocity on Screech in 20,000-Pound Hydrogen-Oxygen Rocket Engine", NASA TN D-3375 (April 1966).
2. Anon., J-2 Quarterly Progress Report for period ending 31 May 1963, Rocketdyne Division, North American Aviation, Inc., Rep. No. R-2600-11 (June 28, 1963).
3. Scott, H. E., Bloomer, H. E., and Mansour, A. H., "M-1 Engine Subscale Injector Tests", Proposed NASA Technical Note.
4. Wanhainen, J. P., Hannum, N. P., and Russell, L. M., "Evaluation of Screech Suppression Concepts in a 20,000-Pound Thrust Hydrogen-Oxygen Rocket", Proposed NASA Technical Memorandum.
5. Reardon, H., "M-1 Thrust Chamber Transverse Mode Combustion Stability Analysis", Aerojet-General Corp., Rep. TCR 9621-012 (1963).
6. Conrad, E. W., Wanhainen, J. P., and Curley, J. K., "Cooled Baffle Development for M-1 Engine Using a Subscale Rocket Engine", NASA TM X-1267 (October 1966).

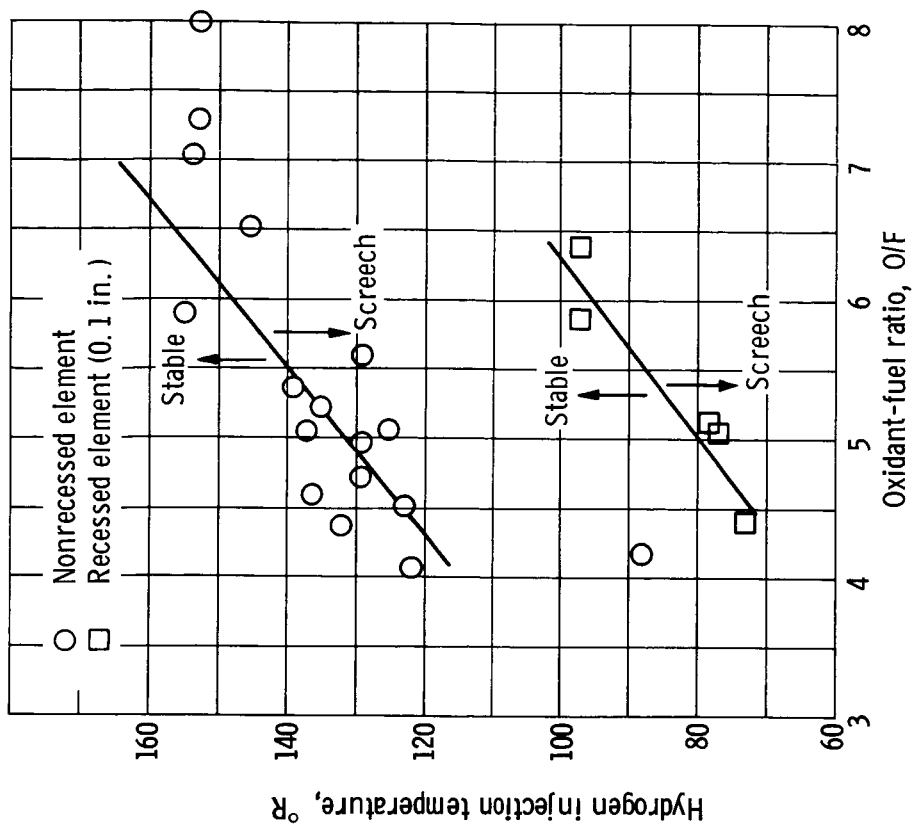


Figure 2. - Effect of oxidizer-tube recess on variation of screech transition temperature. Oxygen area, 0.89 square inch; hydrogen area, 4.84 square inches.

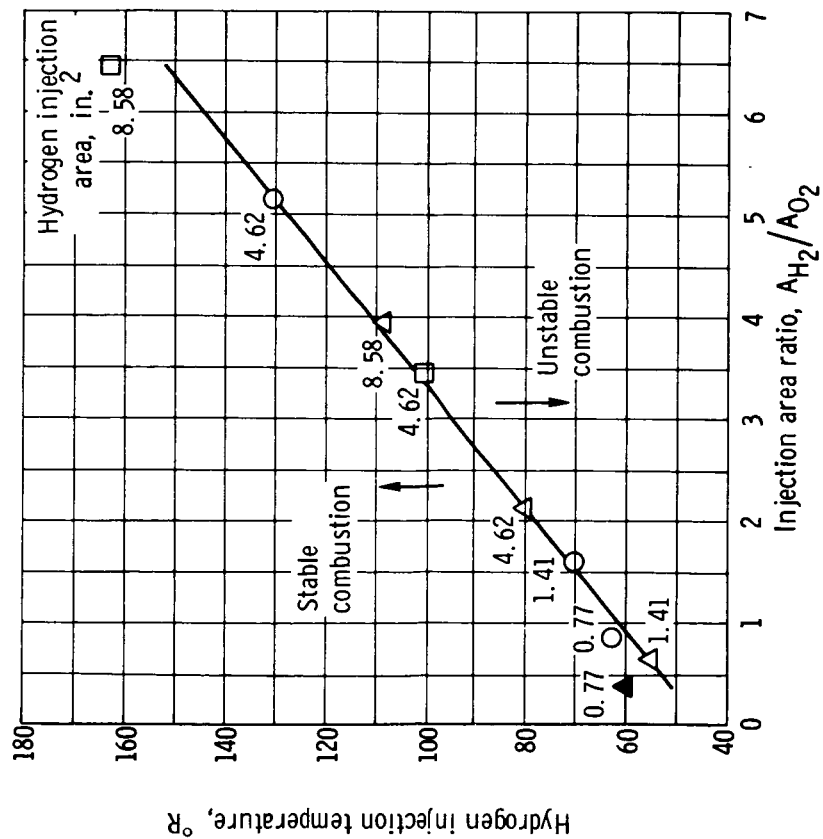
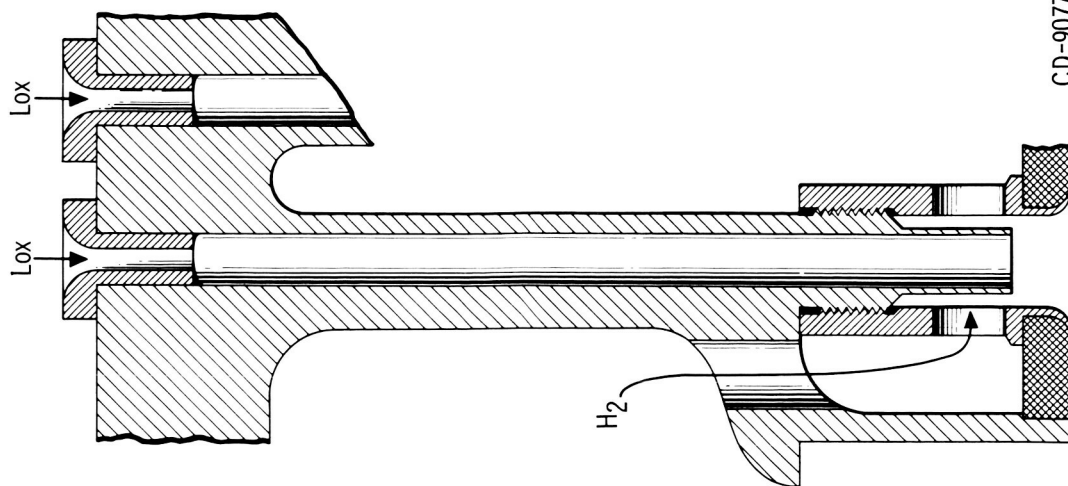


Figure 1. - Correlation of screech transition temperature with injection area ratio for conventional concentric tube element injectors. Oxidant-fuel ratio, 5.



Low  $\Delta P$  fuel  
 FRT prototype  
Type 5939  
 Lox  $\Delta P$  psi 170  
 Fuel  $\Delta P$  psi 90  
 Fuel injection temp. 190 °R  
 Chamber  $\Delta P$  313  
 Film coolant 3% fuel  
 Outer row MR 5.2  
 Area ratio  $A_f/A_{ox}$  1.5  
 Vel. ratio  $V_f/V_{ox}$   
 190°R 12.5  
 At s. t. temp. 2.6  
 Self triggering temp. ~70 °R

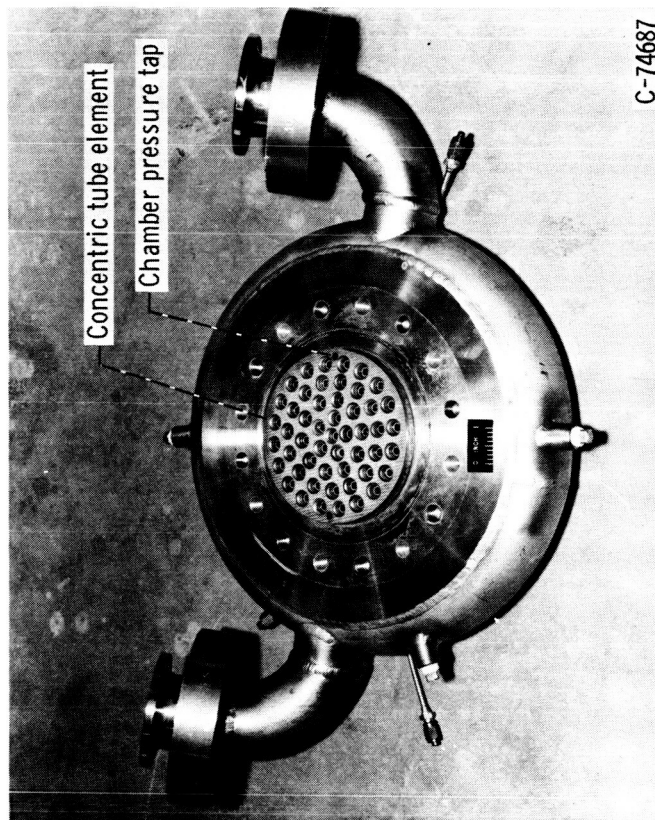
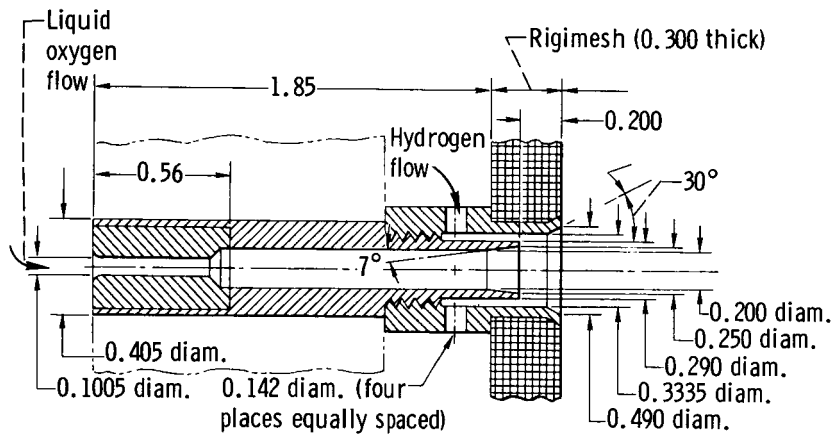
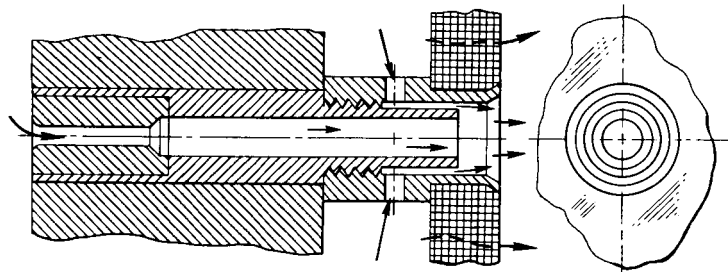


Figure 4. - Subscale injector.

Figure 3. - J-2 injector element.



(a) Prototype design with taper reamed oxidizer tube exit.



(b) Oxidizer tubes with straight bore.

CD-8450

Figure 5. - Cross-sectional view of subscale injector elements.  
(All dimensions are in inches unless otherwise noted.)

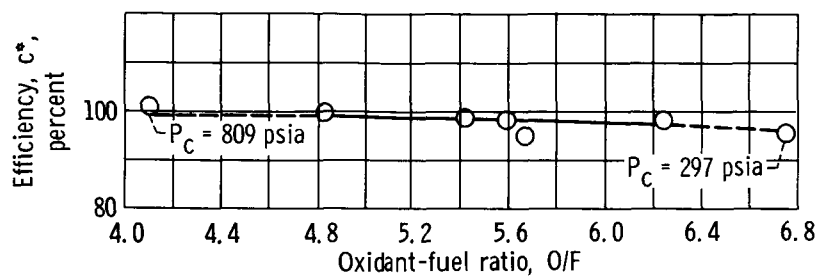


Figure 6. - Subscale injector performance (taper reamed configuration).

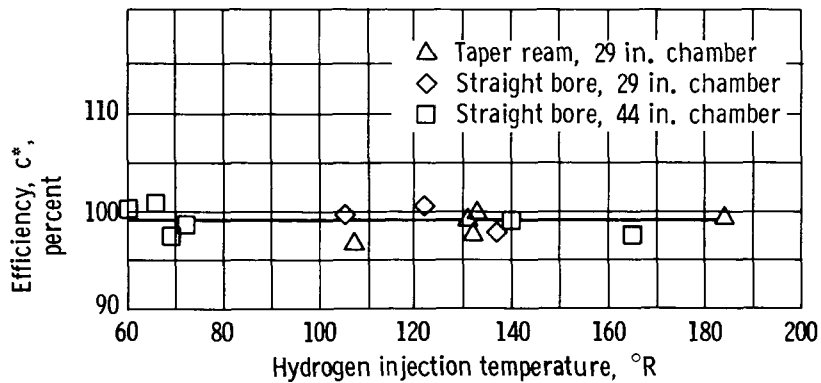
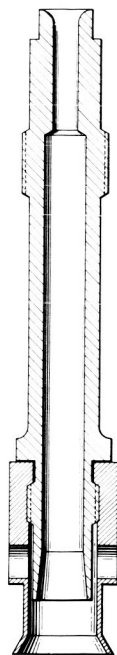


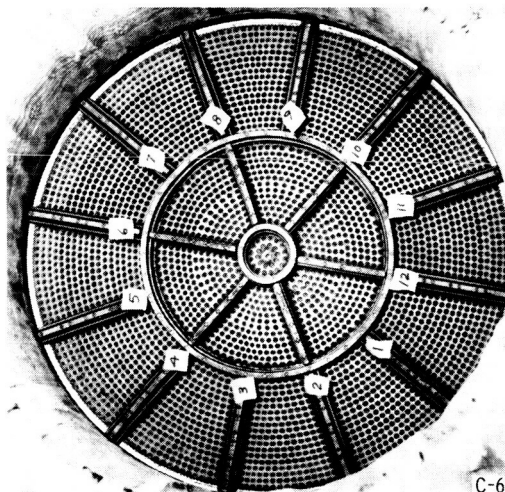
Figure 7. - Subscale injector performance.



Fuel sleeve I. D.	0.333 in.
Ox tube O. D.	0.290 in.
Ox tube I. D.	0.250 in.
Ox tube recess	0.24 in.
Fuel exit area	0.002125 in. <sup>2</sup>
Ox exit area	0.00491 in. <sup>2</sup>
Ox orifice diam.	0.0994-0.1005
Fuel $\Delta P$	140 psi
Ox $\Delta P$	360 psi
Fuel density	1.48 lb/ft <sup>3</sup>
Ox density	70.0 lb/ft <sup>3</sup>
$w_f$ /element	0.133 lb/sec
$w_{ox}$ /element	0.839 lb/sec
$A_f/A_{ox}$	0.433
Fuel velocity	590 ft/sec
Ox velocity	35.2 ft/sec
$V_f/V_{ox}$	17.3

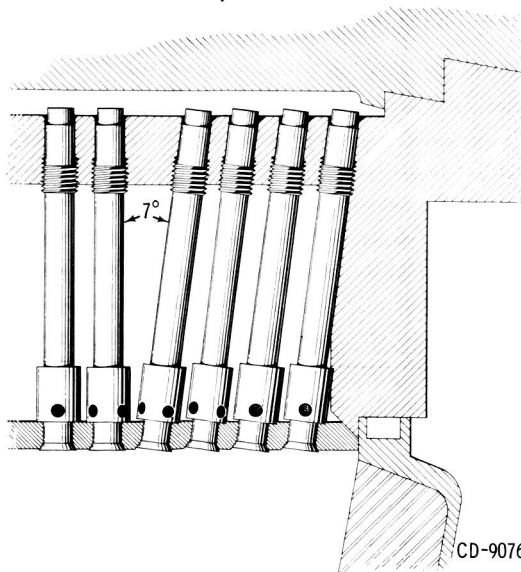
CD-9075

Element detail



C-67-1567

Injector face



CD-9076

Detail showing 4 canted rows

Figure 8. - Full scale injector.



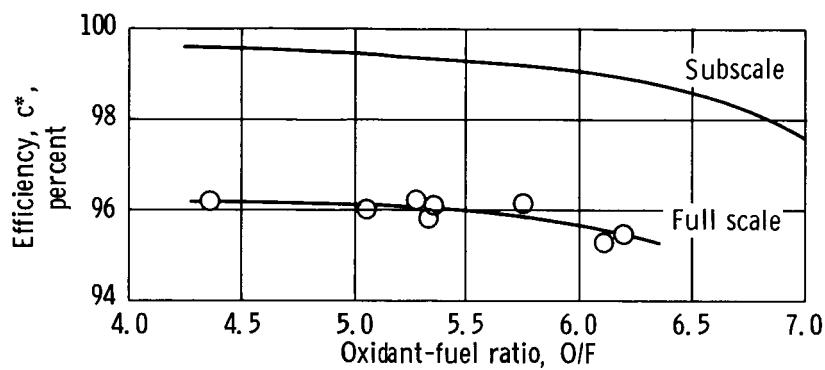


Figure 9. - M-1 thrust chamber  $c^*$  Efficiency against oxidant fuel ratio.

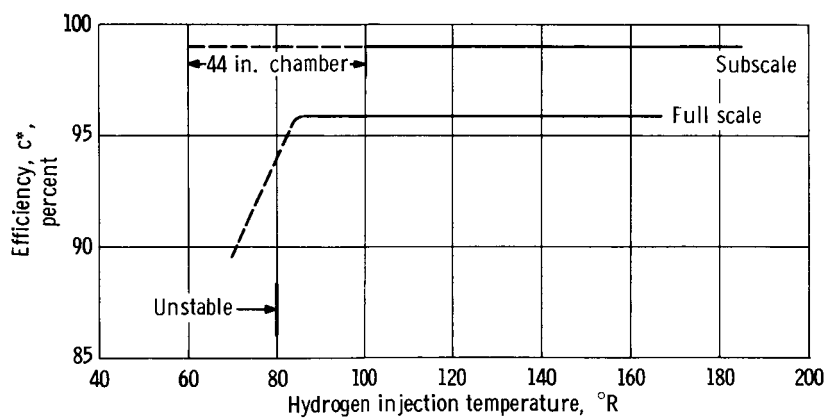


Figure 10. - M-1 thrust chamber  $c^*$  Efficiency against  $\text{H}_2$  injection temperature; O/F =  $5.5 \pm 1.0$ .

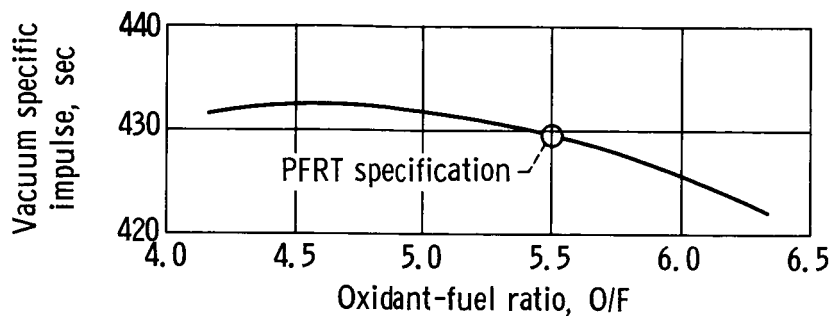


Figure 11. - M-1 thrust chamber vacuum specific impulse against oxidant fuel ratio.  $P_c = 1000$  psia;  $A_e/A_t = 40.0$ ;  $T_{H_2} = 140^\circ R$ .

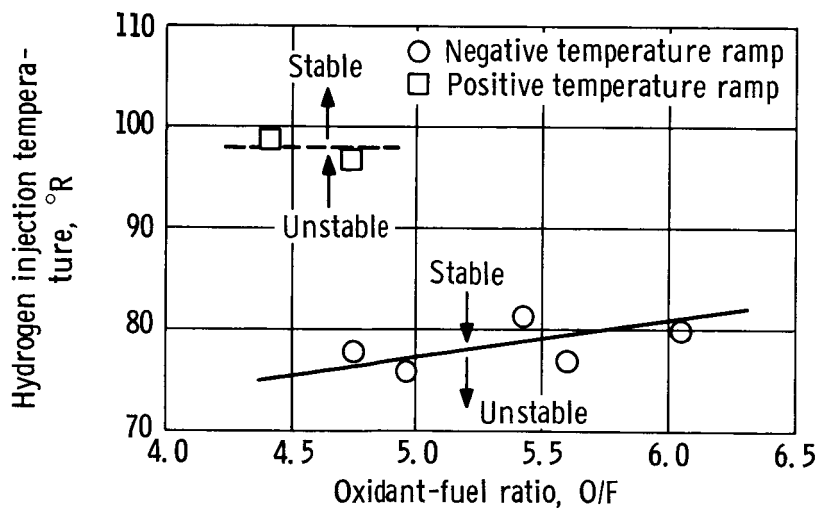


Figure 12. - M-1 thrust chamber combustion stability limits.

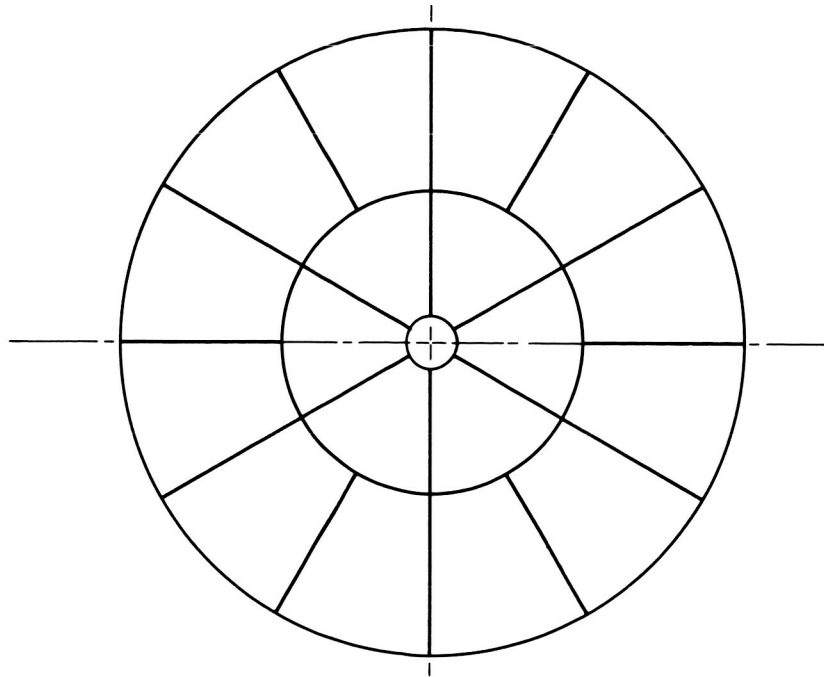


Figure 13. - Recommended baffle configuration.

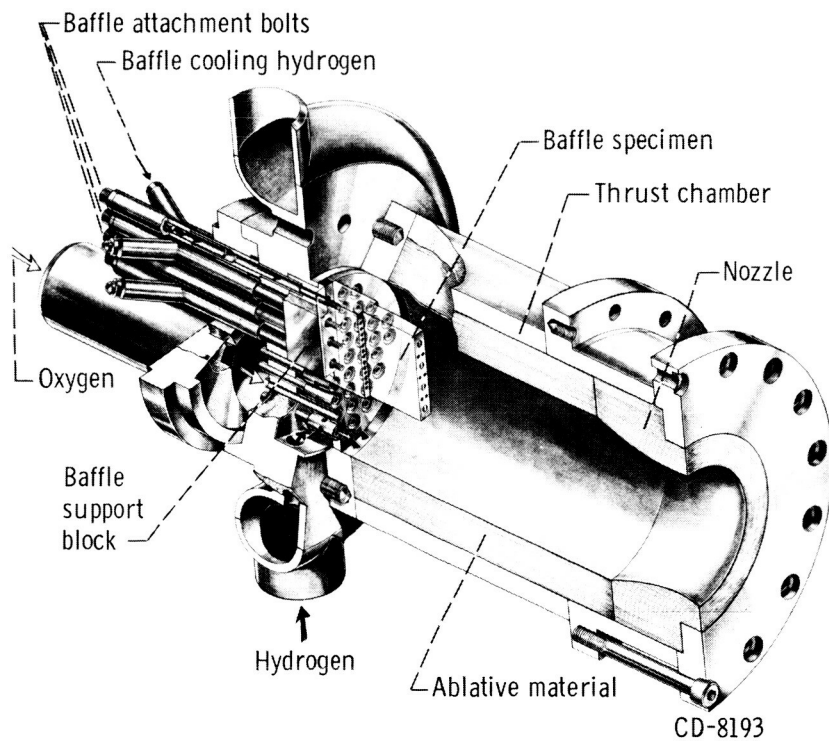


Figure 14. - Cutaway drawing of sub scalp engine.

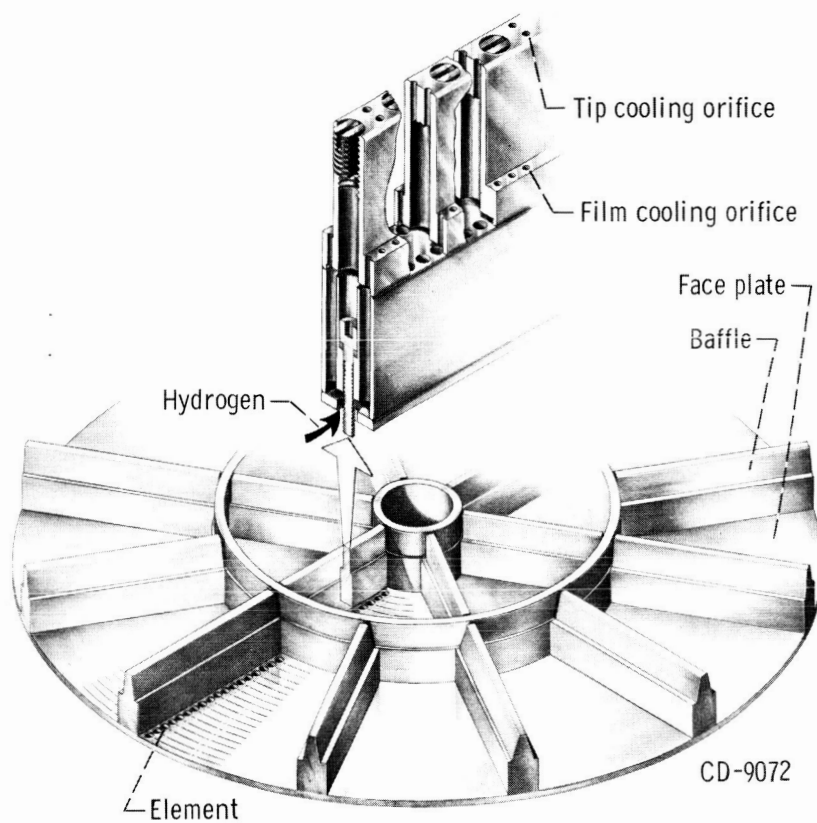
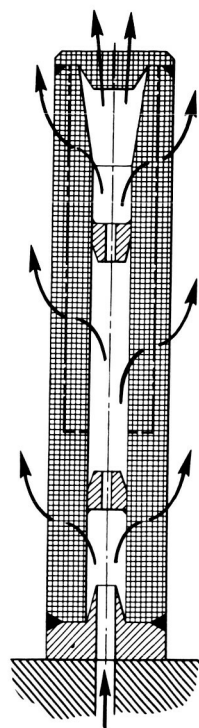
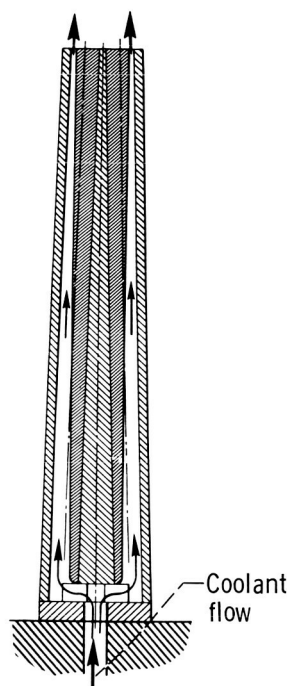


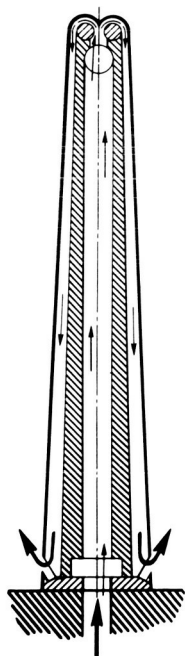
Figure 15. - Layout of full scale M-1 engine baffle.



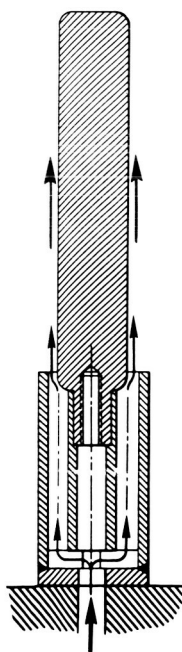
(a) Transpiration.



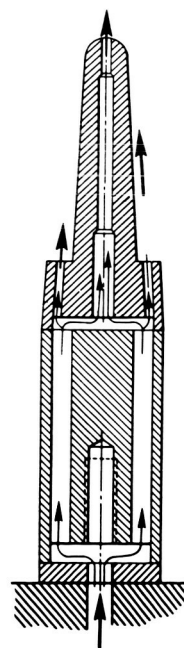
(b) Convection ("dump").



(c) Reverse flow convection.



(d) Film.



(e) Film and convection.

CD-8451

Figure 16. - Baffle cooling concepts investigated.

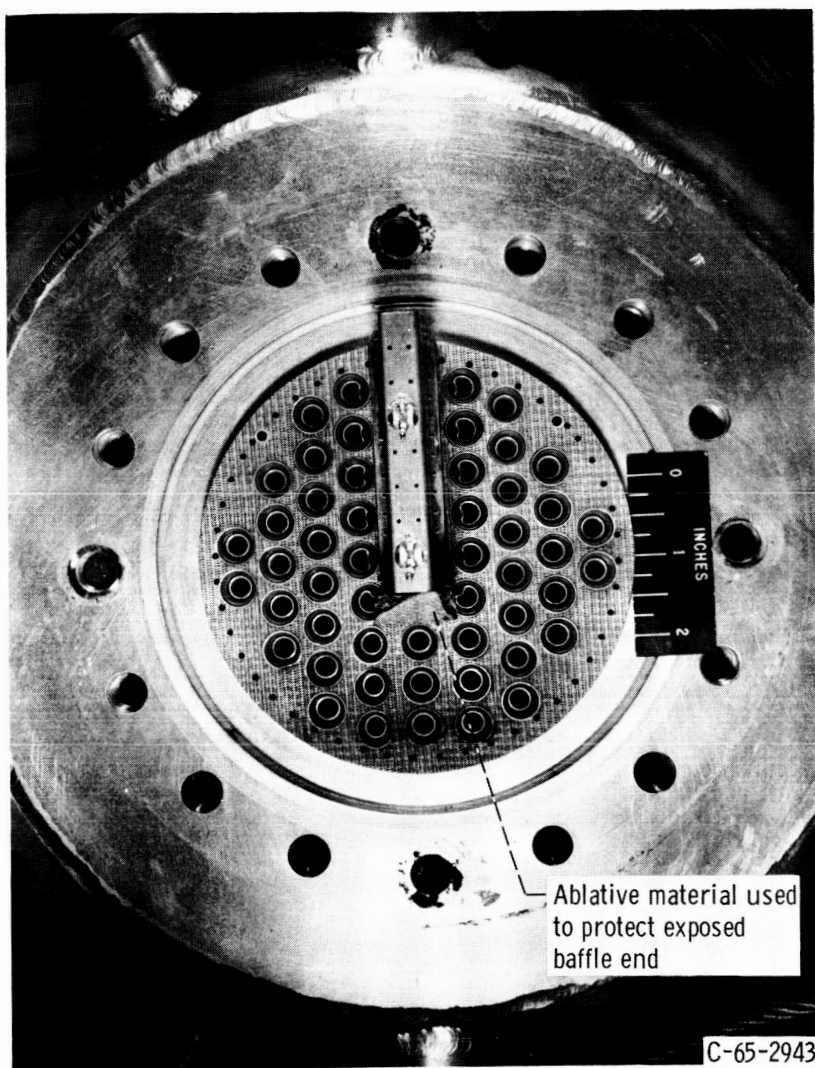


Figure 17. - Subscale injector showing "dimpled" elements adjacent to baffle.

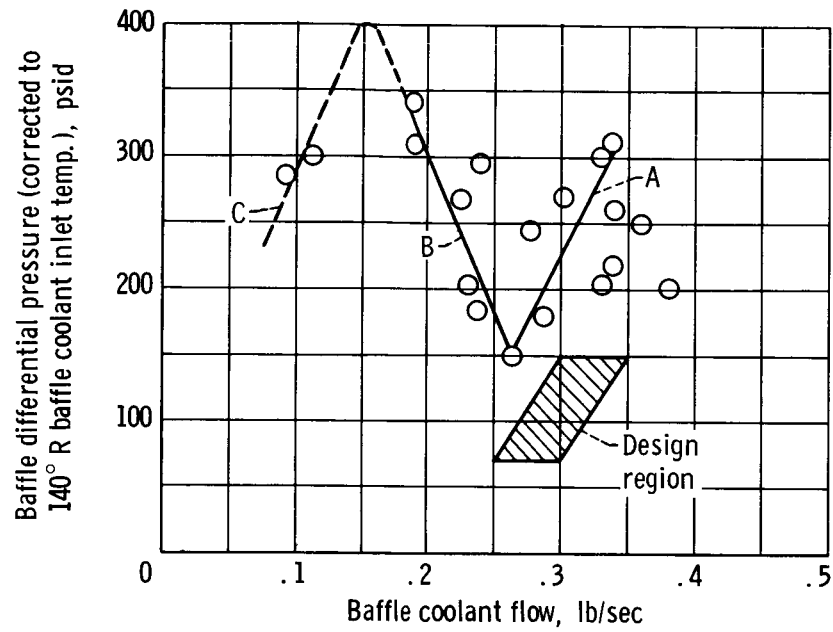


Figure 18. - Flow characteristics of transpiration cooled baffles.

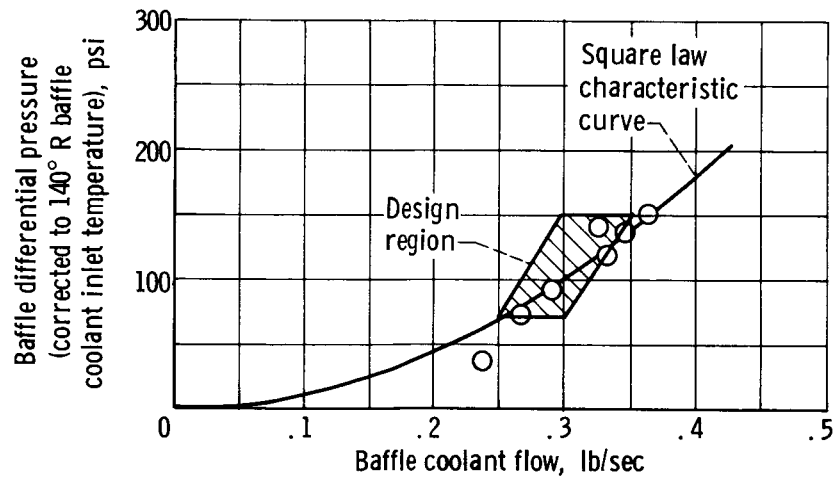


Figure 19. - Flow characteristics of the prototype (copper, convective-film cooled) baffle.

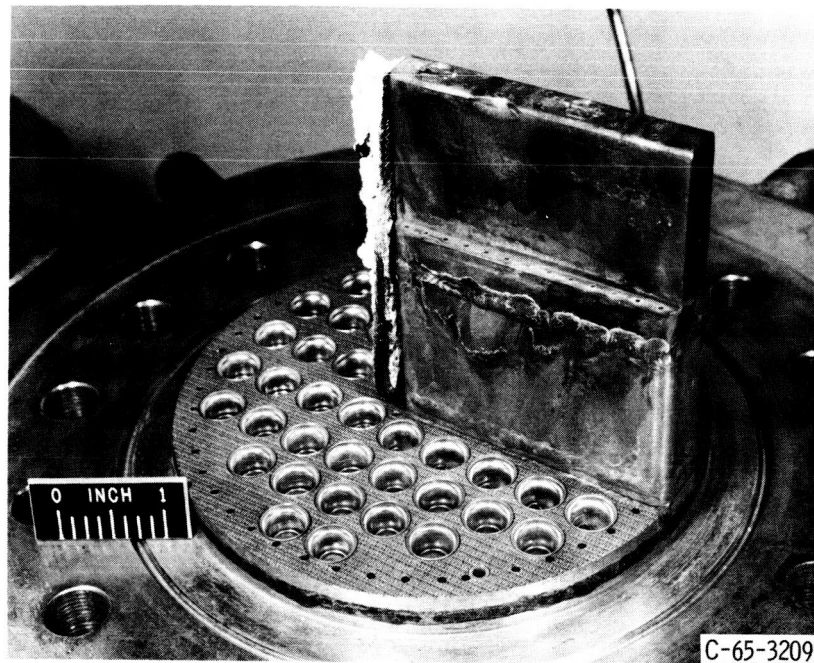


Figure 20. - (a) Post fire condition of prototype baffle after 10 seconds of operation at the lower limit of design coolant flow.

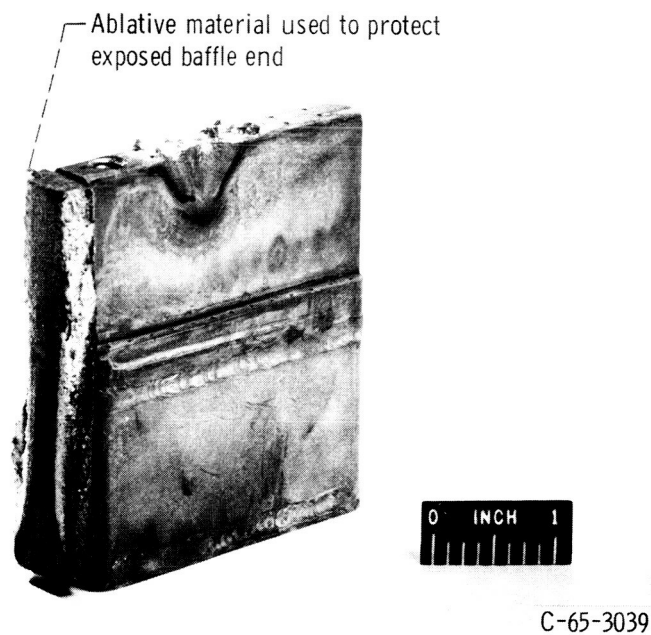


Figure 20. - (b) Post fire condition of prototype baffle after 10 seconds of operation at 80% of lower design flow limit.



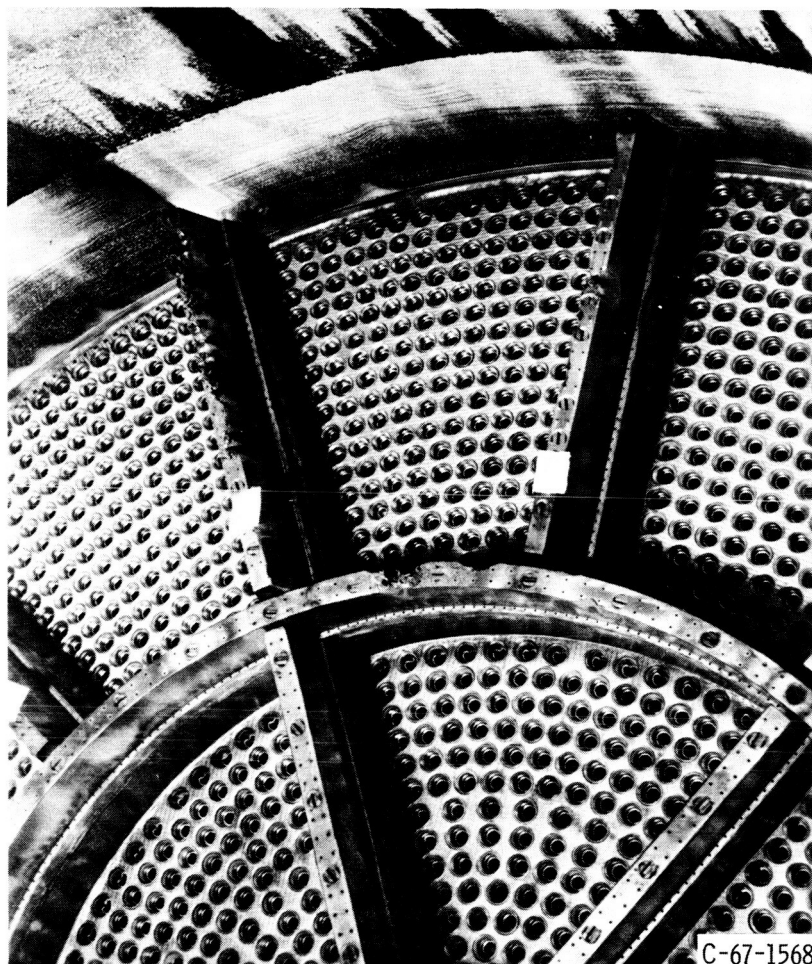


Figure 2I. - Post fire condition of full scale baffle.